Three-dimensional array of dielectric spheres with an isotropic negative permeability at infrared frequencies

Mark S. Wheeler,* J. Stewart Aitchison, and Mohammad Mojahedi

The Edward S. Rogers Sr. Department of Electrical and Computer Engineering, University of Toronto, 10 King's College Road, Toronto, Ontario, Canada M5S 3G4

A negative effective permeability is shown to exist at infrared frequencies in a three-dimensional collection of polaritonic spheres. This is demonstrated by an effective medium theory which relates the Mie resonances of the constituent spheres to the bulk response of the composite. The derived permittivity and permeability are shown to be isotropic. The results are verified by a comparison with multiple-scattering photonic band calculations. The existence of an anomalous dispersion region with a negative group velocity and the appropriate signs associated with the imaginary parts of the permittivity and permeability are also discussed.

PACS number(s): 78.20.Ci, 41.20.Jb, 75.75.+a, 77.84.Lf

I. INTRODUCTION

The recent interest in negative index of refraction metamaterials[1] and their exciting applications, such as the perfect lens,[2] have revived research in the design of artificial dielectrics. The initial negative index metamaterials paired a negative effective permittivity with a negative effective permeability. A negative index has also been demonstrated in loaded transmission line media,[3,4] and a related effect has been found to occur in photonic crystals.[5,6] Experimental results verifying negative refraction in the GHz range have also been reported.[7]

Despite the excellent progress of research on these metamaterials at microwave frequencies, we are interested in designing simpler structures for use at infrared and optical frequencies. For instance, the split-ring resonators (SRRs),[8] which provide a negative effective permeability, have a detailed geometry which becomes difficult to fabricate on a micron scale. Moreover, an SRR only contributes to the negative permeability when the magnetic field is polarized along its axis, meaning that a metamaterial with an isotropic negative permeability would require three orthogonal orientations of SRRs. In contrast, photonic crystal designs[5,6] may be more simple geometrically, but the negative refraction effect is different. In this case, the required Bragg scattering results in practical difficulties such as anisotropy, mode coupling mismatches, and high-order diffraction.[6] Additionally, the fact that the wavelength is on the order of the lattice constant means that these PCs can only be used in a limited way for device miniaturization. Lastly, the transmission line media seem to be unsuitable for the infrared because of the need for lumped components or intricate printed loading elements.

An alternate method of producing a negative permeability is to use the Mie resonances of dielectric spheres. Spheres with large values of permittivity have leaky cavity resonances at frequencies where the corresponding wavelength in the ambient medium remains much larger than the size of the spheres. A large collection of such spheres can be described by an effective permeability; a strong enough resonance creates a negative permeability. The effective permittivity and permeability of arbitrary spheres was considered by Lewin.[9] This work was extended recently in reports of

negative index metamaterials that used interpenetrating arrays of magnetodielectric[10] and ferroelectric[11] spheres. Similar effective medium theories also have been reported.[12,13] Finally, just prior to the submission of this paper we have become aware of the publication of Ref. 14, which is similar to the present report, and verifies some of our results shown here and elsewhere.[15] There are also other reports of a negative index of refraction that rely on Mie resonances, but either depend solely on the electric dipole resonance,[16] or require quadrupole resonances.[17]

In a report independent of the previous references, O'Brien and Pendry[18] showed that a two-dimensional array of ferroelectric rods has a negative effective permeability in the GHz range when the magnetic field is polarized along the axes of the rods. It was subsequently shown that polaritonic rods can be used to extend this concept to the infrared in two dimensions.[19] Although the underlying physics is the same, these reports used an alternate method to find the effective media values. The validity of this method is discussed later in this paper.

We report a three-dimensional collection of polaritonic, nonmagnetic spheres with a negative effective permeability at infrared frequencies. In addition, this effective permeability is shown to be isotropic for modest filling fractions. Section II summarizes the simple yet rigorous effective medium theory used to calculate the effective electromagnetic parameters. Section III presents the effective permeability and permittivity calculated for a collection of LiTaO$_3$ spheres. A scattering matrix technique is then used to calculate the band structure of an equivalent periodic structure, which further verifies the results of the effective medium theory. We comment on the resulting negative group velocity, and contrast the effective media theory with other methods. Finally, we summarize the results in Sec. IV.

II. EFFECTIVE MEDIUM THEORY

Consider a single isolated dielectric sphere of radius r_0 and relative permittivity $\epsilon_r = n^2$. A plane wave, which has a magnetic field $\mathbf{H}_{inc} = H_0 \exp(ik_0z)\hat{\mathbf{y}}$ where $k_0 = \omega/c$, is incident on the sphere. The scattered field can be decomposed into a multipole series,[20] with the 2^m-pole term of the magnetic field proportional to

$$b_m = \frac{\psi_m(nx)\psi_m'(x) - n\psi_m(x)\psi_m'(nx)}{\psi_m(nx)\xi_m'(x) - n\xi_m(x)\psi_m'(nx)}, \tag{1}$$

whereas the 2^m-pole term of the scattered electric field is proportional to

$$a_m = \frac{n\psi_m(nx)\psi_m'(x) - \psi_m(x)\psi_m'(nx)}{n\psi_m(nx)\xi_m'(x) - \xi_m(x)\psi_m'(nx)}. \tag{2}$$

Here $x = k_0 r_0$, and $\psi_m(x)$ and $\xi_m(x)$ are the Riccati-Bessel functions,[21] and the primes indicate differentiation with respect to the argument. Only the b_1 coefficient, which is the strength of the magnetic dipole response, will be of interest when considering the effective permeability; only the a_1 term will be needed to find the effective permittivity.

Near the lowest resonant frequency of b_1, the sphere is equivalent to a magnetic dipole. The dominant contribution to the scattered magnetic field is then due to only the dipole term,

$$\mathbf{H}_{\text{sca}} = \frac{3i}{2} H_0 b_1 \frac{e^{ik_0 r}}{k_0 r} [(\hat{\mathbf{y}} \cdot \hat{\boldsymbol{\theta}})\hat{\boldsymbol{\theta}} + (\hat{\mathbf{y}} \cdot \hat{\boldsymbol{\varphi}})\hat{\boldsymbol{\varphi}}]$$

$$= -\frac{3i}{2} H_0 b_1 \frac{e^{ik_0 r}}{k_0 r} \hat{\mathbf{r}} \times (\hat{\mathbf{r}} \times \hat{\mathbf{y}}), \tag{3}$$

in the far field.[20] If the free-space wavelength is much larger than the diameter of the sphere, the sphere may be replaced conceptually by a radiating magnetic dipole of moment $\mathbf{m}$. The radiated field must then match the standard far-field expression of dipole radiation,[22]

$$\mathbf{H}_{\text{dipole}} = -\frac{k_0^3}{4\pi} \frac{e^{ik_0 r}}{k_0 r} \hat{\mathbf{r}} \times (\hat{\mathbf{r}} \times \mathbf{m}). \tag{4}$$

Equating (3) and (4) provides the equivalent magnetic dipole moment of a single dielectric sphere, in terms of its b_1 scattering coefficient.[12] The induced magnetic dipole moment is related to the incident wave by $\mathbf{m} = \alpha_m \mathbf{H}_{\text{inc}}(z=0)$, where α_m is the magnetic polarizability.

The effective permeability μ_r^{eff} must describe the response of a large collection of such magnetic dipoles. This is done by averaging the fields in the long-wavelength limit. The magnetic polarizability can be related to the effective permeability by using the Clausius-Mossotti equation,[22]

$$\alpha_m = \frac{3}{N}\left(\frac{\mu_r^{\text{eff}} - 1}{\mu_r^{\text{eff}} + 2}\right), \tag{5}$$

where N is the volume density of the dipoles. The filling fraction f of the composite is $f = 4\pi N r_0^3/3$, and should be kept to modest values. The effective permeability is then

$$\mu_r^{\text{eff}} = \frac{k_0^3 + 4\pi i N b_1}{k_0^3 - 2\pi i N b_1}. \tag{6}$$

Similarly, the effective permittivity ϵ_r^{eff} is due to the scattered electric dipole term a_1, and is given by

$$\epsilon_r^{\text{eff}} = \frac{k_0^3 + 4\pi i N a_1}{k_0^3 - 2\pi i N a_1}. \tag{7}$$

Equations (6) and (7), along with (1) and (2), determine the effective electromagnetic parameters in the long-wavelength limit. The forms of (6) and (7), also found in Ref. 13, are equivalent to the formulation of Lewin[9] and other reports.[10,11]

III. NEGATIVE PERMEABILITY

A. Magnetic resonance of polaritonic spheres

The magnetic dipole response is usually weak. This can be driven into resonance, however, by using materials with a large permittivity, such as ferroelectrics.[11,18] However, their extreme permittivity drops off before infrared frequencies. Instead, the polaritonic resonances of crystals, or *reststrahlen* region, can serve this purpose in the infrared.[19] The large dielectric permittivity of the spheres also aids in scaling the resonances into the long-wavelength limit. Polaritonic materials have a relative permittivity

$$\epsilon_r(\omega) = \epsilon(\infty)\left(1 + \frac{\omega_L^2 - \omega_T^2}{\omega_T^2 - \omega^2 - i\omega\gamma}\right), \tag{8}$$

where $\epsilon(\infty)$ is the high-frequency limit of the permittivity, ω_T is the transverse optical phonon frequency, ω_L is the longitudinal optical phonon frequency, and γ is the damping coefficient.[23] These parameters are related by the Lyddane-Sachs-Teller relation $\omega_L^2/\omega_T^2 = \epsilon(0)/\epsilon(\infty)$, where $\epsilon(0)$ is the static permittivity. We choose to use the crystal LiTaO$_3$, the same as considered in Ref. 19. The parameters used in our calculations are $\epsilon(0) = 41.4$, $\epsilon(\infty) = 13.4$, $\omega_T/2\pi = 4.25$ THz, $\omega_L/2\pi = 7.46$ THz, and $\gamma/2\pi = 0.15$ THz. It should also be noted that these values, which are taken from experimental results,[24] do not match those stated in Ref. 19; the latter frequencies are a factor of 2π too large.

We choose spheres of LiTaO$_3$ because of its large static permittivity $\epsilon(0)$. It is the large dielectric constant, and not necessarily the material resonance, which drives a strong resonance in the magnetic dipole moment of the spheres, and makes it easier to create a negative effective permeability.

The effective permeability of a collection of LiTaO$_3$ spheres is shown in Fig. 1(a), and the effective permittivity is shown in Fig. 1(b). The radius of the spheres is 4 μm. The filling fraction is 26.81%, which corresponds to the periodic structure that will be used later to verify these effective parameters. The free-space wavelength at the permeability resonance exceeds the diameter of the spheres by a factor of 10.6, which affirms the validity of the long-wavelength approximation used to calculate the effective medium values.

The resonance in the effective permeability shown in Fig. 1(a) at 3.53 THz is below the transverse phonon frequency ($\omega_T/2\pi = 4.25$ THz) and happens to be, as expected, in the range where the material permittivity grows quite large. The effective permeability becomes negative just above this resonance. The effective permittivity shown in Fig. 1(b) has a very weak resonance at 3.9 THz. In addition, a strong resonance and negative permittivity occurs near 6.77 THz [not shown in Fig. 1(b)], although at such high frequencies the long-wavelength approximation begins to break down.

The imaginary parts of both the calculated effective permeability and permittivity are always positive. This indicates attenuation, either due to material losses or reactive energy storage. Interestingly, a number of researchers have calculated the effective permittivity and permeability for other metamaterials, and in some cases have found a negative imaginary permittivity,[18,19,25] which on its own would indicate gain from a passive structure. Nonetheless, the fundamental difference between our results and others is in the
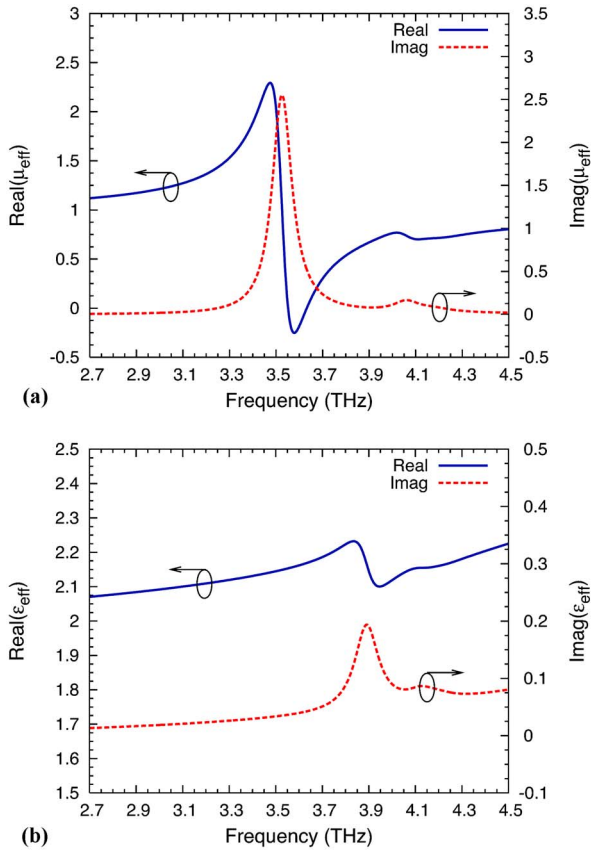
FIG. 1. (Color online) The effective relative permeability (a) and permittivity (b) of a collection of LiTaO$_3$ spheres. The radius of the spheres is 4 μm. The filling fraction is 26.81%.
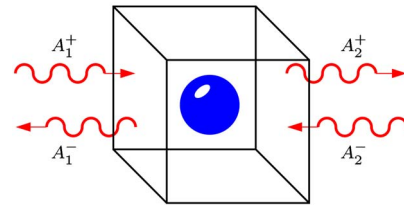

FIG. 2. (Color online) A unit cell of the simple cubic crystal, indicating the components of the scattered waves. This figure assumes propagation along the ΓX direction.

This program finds the complex band structure of a three-dimensional photonic crystal by calculating the scattering within a two-dimensional plane of spheres, and then uses Bloch's theorem along the third dimension of periodicity to calculate the longitudinal dispersion relation. The mode frequency is the independent variable. A scattering matrix approach relates the fields on the two ends of a unit cell in the direction of propagation, according to

$$\mathbf{A}_2^+ = \mathbf{T}_{21} \cdot \mathbf{A}_1^+ + \mathbf{R}_{22} \cdot \mathbf{A}_2^-,$$

$$\mathbf{A}_1^- = \mathbf{R}_{11} \cdot \mathbf{A}_1^+ + \mathbf{T}_{12} \cdot \mathbf{A}_2^-, \tag{9}$$

where $\mathbf{A}_i^\pm$ are column vectors representing the components of the fields, as defined in Fig. 2. The $\mathbf{T}_{ij}$ and $\mathbf{R}_{ij}$ are transmission and reflection matrices from the jth to ith plane, and include all of the information regarding the lattice, sphere

method of calculation of the effective medium values. In the other reports, the permeability and permittivity are found from calculations of the effective index and reflectance. The index is taken from band structure calculations, and the reflectance is calculated for a slab of finite thickness L. However, the effective media values should not depend on L. This assumption makes the results ambiguous and perhaps leads to the negative imaginary permittivity in the aforementioned references. On the other hand, the direct calculation using analytical field expressions and the Clausius-Mossotti equation, applied here, results in the strictly positive imaginary values shown in Figs. 1(a) and 1(b).

B. Isotropy and verification

The effective permeability and permittivity that have been found are only strictly true in the long-wavelength limit. The actual arrangement of the spheres, particularly a periodic lattice arrangement, will have little impact on the effective dispersion, resulting in isotropic effective values. This assertion can be verified by a comparison with a full multiple scattering approach, which takes into account the interactions between the spheres, as well as higher multipole contributions. The previous discussion on the imaginary parts of the effective values also reveals the need for further verification. Therefore, we performed photonic crystal band calculations using modifications of the code MULTEM2 from Ref. 26.
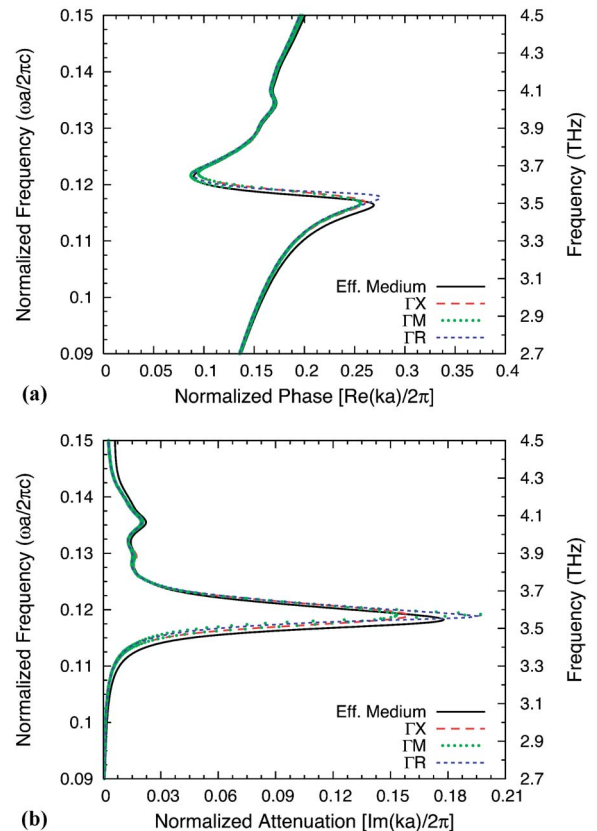

FIG. 3. (Color online) The eigenfrequencies of a simple cubic lattice of LiTaO$_3$ spheres, as a function of the real part (a), and imaginary part (b) of the Bloch wave vector. The lattice constant is $a=10$ μm and the radius of the spheres is $r_0=0.4a$.

size, sphere and host dielectrics, frequency, and transverse wave vector. The Bloch condition is imposed along the direction of propagation, so that $\mathbf{A}_2^{\pm} = \exp(ika)\mathbf{A}_1^{\pm}$, where k is the longitudinal component of the Bloch wave vector, and a is the unit cell size. This code then solves the eigenvalue problem

$$e^{ika}\begin{bmatrix} \mathbf{I} & \mathbf{0} \\ \mathbf{R}_{11} & \mathbf{T}_{12} \end{bmatrix}\begin{bmatrix} \mathbf{A}_1^+ \\ \mathbf{A}_2^- \end{bmatrix} = \begin{bmatrix} \mathbf{T}_{21} & \mathbf{R}_{22} \\ \mathbf{0} & \mathbf{I} \end{bmatrix}\begin{bmatrix} \mathbf{A}_1^+ \\ \mathbf{A}_2^- \end{bmatrix}, \quad (10)$$

where $\mathbf{I}$ is the identity matrix. The only approximations are in the angular momentum cutoff in the spherical scattering coefficients and the number of reciprocal lattice vectors taken in each two-dimensional plane of spheres. We have modified the code to accommodate the dispersive polaritonic materials of the spheres.

A simple cubic lattice is chosen to verify the effective medium approach. The lattice constant is $a = 10$ μm, and the LiTaO$_3$ spheres have a radius of $r_0 = 0.4a$. This corresponds to a filling fraction of 26.81% (using $N = 1/a^3$) which is the same value used in our effective medium approach. The Bloch wave vector was calculated along the ΓX, ΓM, and ΓR directions. The results are shown in Fig. 3(a). These are compared with the effective photon dispersion, which is given by the relation

$$k = k' + ik'' = \frac{\omega}{c}\sqrt{\epsilon_r^{\text{eff}}(\omega)\mu_r^{\text{eff}}(\omega)}, \quad (11)$$

in the long-wavelength limit, and ensuring that $k'' \geqslant 0$. The isotropic response of the composite is verified by the closely matching curves. Note that the two nondegenerate modes for the ΓM direction can be distinguished on careful inspection, although the code does not converge well for one of these modes at the center of the resonance. At frequencies slightly beyond the range of the figure, the long-wavelength approximation starts to break down and the curves begin to differ. The comparison in Fig. 3(a) indicates that the calculated ef-fective parameters indeed do describe the wave propagation in the composite.

The main interesting feature in the band structure, which is the "kink" centered at $\omega a/2\pi c = 0.118$, is due to the resonance in the effective permeability. This is an anomalous dispersion region, in which the group velocity is negative, $v_g = \partial\omega/\partial k < 0$. A negative group velocity means that the group delay of a pulse traveling through the structure is negative, i.e., the peak of the output pulse *precedes* the peak of the input pulse.[27] This does not, however, violate causality, as long as passive media display attenuation in the anomalous dispersion region.[4,28] The attenuation of the present composite is shown in Fig. 3(b) as the imaginary part of the Bloch wave vector, which manifests itself as a pseudogap. Note that this is an entirely different effect than a Bragg resonance, and as such the phase shown in Fig. 3(a) varies in the gap.

IV. SUMMARY

We have presented a metamaterial composed of polaritonic spheres which has a negative effective permeability at infrared frequencies. The three-dimensional, isotropic magnetic response is controlled by the size, density, and dielectric properties of the spheres. This composite has a very simple structure, and is a viable alternative to SRRs. It may also be used to extend paramagnetic and diamagnetic materials to optical frequencies.

ACKNOWLEDGMENT

*Email address: mark.wheeler@utoronto.ca

[1] D. R. Smith *et al.*, Phys. Rev. Lett. **84**, 4184 (2000).

[2] J. B. Pendry, Phys. Rev. Lett. **85**, 3966 (2000).

[3] G. V. Eleftheriades *et al.*, IEEE Trans. Microwave Theory Tech. **50**, 2702 (2002).

[4] O. F. Siddiqui *et al.*, IEEE Trans. Antennas Propag. **51**, 2619 (2003).

[5] M. Notomi, Phys. Rev. B **62**, 10696 (2000).

[6] M. S. Wheeler *et al.*, Phys. Rev. B **71**, 155106 (2005).

[7] R. A. Shelby *et al.*, Science **292**, 77 (2001).

[8] J. B. Pendry *et al.*, Phys. Rev. Lett. **76**, 4773 (1996).

[9] L. Lewin, Proc. Inst. Electr. Eng. **94**, 65 (1947).

[10] C. L. Holloway *et al.*, IEEE Trans. Antennas Propag. **51**, 2596 (2003).

[11] O. G. Vendik and M. S. Gashinova, in *Proceedings of the 34th European Microwave Conference, Amsterdam* (IEEE Press, Piscataway, NJ, 2004), Vol. 3, pp. 1209–1212.

[12] W. T. Doyle, Phys. Rev. B **39**, 9852 (1989).

[13] C. A. Grimes and D. M. Grimes, Phys. Rev. B **43**, 10780 (1991).

[14] V. Yannopapas and A. Moroz, J. Phys.: Condens. Matter **17**, 3717 (2005).

[15] M. S. Wheeler, J. S. Aitchison, and M. Mojahedi, in *Proceedings of IASTED Conf. on Antennas, Radar, and Wave Propagat., Banff, Canada* (Acta Press, Calgary, AB, Canada, 2005), 475-143.

[16] A. Alù, A. Salandrino, and N. Engheta, cond-mat/0412263.

[17] G. Shvets and Y. A. Urzhumov, Phys. Rev. Lett. **93**, 243902 (2004).

[18] S. O'Brien and J. B. Pendry, J. Phys.: Condens. Matter **14**, 4035 (2002).

[19] K. C. Huang *et al.*, Appl. Phys. Lett. **85**, 543 (2004).

[20] C. F. Bohren and D. R. Huffman, *Absorption and Scattering of Light by Small Particles* (Wiley-Interscience, New York, 1983).

[21] *Handbook of Mathematical Functions with Formulas, Graphs, and Mathematical Tables*, edited by M. Abramowitz and I. A. Stegun (Dover, New York, 1972).

[22] J. D. Jackson, *Classical Electrodynamics*, 3rd ed. (John Wiley and Sons Inc., New York, 1999).

[23] C. Kittel, *Introduction to Solid State Physics*, 7th ed. (John Wiley and Sons Inc., New York, 1996).

[24] M. Schall *et al.*, Int. J. Infrared Millim. Waves **20**, 595 (1999).

[25] T. Koschny *et al.*, Phys. Rev. E **68**, 065602(R) (2003).

[26] N. Stefanou *et al.*, Comput. Phys. Commun. **132**, 189 (2000).

[27] J. F. Woodley and M. Mojahedi, Phys. Rev. E **70**, 046603 (2004).

[28] M. Mojahedi *et al.*, Phys. Rev. E **62**, 5758 (2000).